



Characterization of SARS-CoV-2 Variants B.1.617.1 (Kappa), B.1.617.2 (Delta), and B.1.618 by Cell Entry and Immune Evasion

Wenlin Ren,^a Xiaohui Ju,^a Mingli Gong,^a Jun Lan,^b Yanying Yu,^a  Quanxin Long,^c Devin J. Kenney,^{d,e} Aoife K. O'Connell,^{d,e} Yu Zhang,^a  Jin Zhong,^f  Guocai Zhong,^{g,h} Florian Douam,^{d,e} Xinquan Wang,^b Ailong Huang,^c Rong Zhang,ⁱ  Qiang Ding^a

^aCenter for Infectious Disease Research, School of Medicine, Tsinghua University, Beijing, China

^bSchool of Life Sciences, Tsinghua University, Beijing, China

^cKey Laboratory of Molecular Biology on Infectious Diseases, Ministry of Education, Chongqing Medical University, Chongqing, China

^dDepartment of Microbiology, Boston University School of Medicine, Boston, Massachusetts, USA

^eNational Emerging Infectious Diseases Laboratories, Boston University, Boston, Massachusetts, USA

^fUnit of Viral Hepatitis, CAS Key Laboratory of Molecular Virology and Immunology, Institut Pasteur of Shanghai, Chinese Academy of Sciences, Shanghai, China

^gShenzhen Bay Laboratory, Shenzhen, China

^hSchool of Chemical Biology and Biotechnology, Peking University Shenzhen Graduate School, Shenzhen, China

ⁱKey Laboratory of Medical Molecular Virology (MOE/NHC/CAMS), School of Basic Medical Sciences, Shanghai Medical College, Biosafety Level 3 Laboratory, Fudan University, Shanghai, China

Wenlin Ren, Xiaohui Ju, Mingli Gong, Jun Lan, and Yanying Yu contributed equally to this article. Author order was determined based on project leadership.

ABSTRACT Recently, highly transmissible severe acute respiratory syndrome coronavirus 2 (SARS-CoV-2) variants B.1.617.1 (Kappa), B.1.617.2 (Delta), and B.1.618 with mutations within the spike proteins were identified in India. The spike protein of Kappa contains the four mutations E154K, L452R, E484Q, and P681R, and Delta contains L452R, T478K, and P681R, while B.1.618 spike harbors mutations Δ 145–146 and E484K. However, it remains unknown whether these variants have alterations in their entry efficiency, host tropism, and sensitivity to neutralizing antibodies as well as entry inhibitors. In this study, we found that Kappa, Delta, or B.1.618 spike uses human angiotensin-converting enzyme 2 (ACE2) with no or slightly increased efficiency, while it gains a significantly increased binding affinity with mouse, marmoset, and koala ACE2 orthologs, which exhibit limited binding with wild-type (WT) spike. Furthermore, the P681R mutation leads to enhanced spike cleavage, which could facilitate viral entry. In addition, Kappa, Delta, and B.1.618 exhibit a reduced sensitivity to neutralization by convalescent-phase sera due to the mutation E484Q, T478K, Δ 145–146, or E484K, but remain sensitive to entry inhibitors such as ACE2-Ig decoy receptor. Collectively, our study revealed that enhanced human and mouse ACE2 receptor engagement, increased spike cleavage, and reduced sensitivity to neutralization antibodies of Kappa, Delta and B.1.618 may contribute to the rapid spread of these variants. Furthermore, our results also highlight that ACE2-Ig could be developed as a broad-spectrum antiviral strategy against SARS-CoV-2 variants.

IMPORTANCE SARS-CoV-2, the causative agent of pandemic COVID-19, is rapidly evolving to be more transmissible and to exhibit evasive immune properties, compromising neutralization by antibodies from vaccinated individuals or convalescent-phase sera. Recently, SARS-CoV-2 variants B.1.617.1 (Kappa), B.1.617.2 (Delta), and B.1.618 with mutations within the spike proteins were identified in India. In this study, we examined cell entry efficiencies of Kappa, Delta, and B.1.618. In addition, the variants, especially the Delta variant, exhibited expanded capabilities to use mouse, marmoset, and koala ACE2 for entry. Convalescent sera from patients infected with nonvariants showed reduced neutralization titers among the Kappa, Delta, and B.1.618 variants. Furthermore, the variants remain sensitive to ACE2-Ig decoy receptor. Our study thus could facilitate

Editor Xiang-Jin Meng, Virginia Polytechnic Institute and State University

Copyright © 2022 Ren et al. This is an open-access article distributed under the terms of the [Creative Commons Attribution 4.0 International license](https://creativecommons.org/licenses/by/4.0/).

Address correspondence to Qiang Ding, qding@tsinghua.edu.cn.

The authors declare no conflict of interest.

Received 20 January 2022

Accepted 15 February 2022

Published 10 March 2022

understanding how variants have increased transmissibility and evasion of established immunity and also could highlight the use of an ACE2 decoy receptor as a broad-spectrum antiviral strategy against SARS-CoV-2 variants.

KEYWORDS COVID-19, SARS-CoV-2, Delta variant, Kappa variant, B.1.618, ACE2 decoy receptor

Since its emergence in late 2019, severe acute respiratory syndrome coronavirus 2 (SARS-CoV-2), which causes the ongoing COVID-19 pandemic, has evolved into several new viral variants of concern (VOC) and variants of interest (VOI) (1–4). SARS-CoV-2 enters host cells by binding angiotensin-converting enzyme 2 (ACE2) in a species-dependent manner (2, 5, 6). For example, murine, New World monkey, and koala versions of ACE2 do not efficiently bind the SARS-CoV-2 spike protein, hindering viral entry into those species (7). In addition, the spike is the target for vaccine and therapeutic antibodies (8, 9), and mutations in spike may potentially alter SARS-CoV-2 transmission, host tropism, pathogenicity, as well as sensitivity to vaccine-elicited antibodies (10–12). For example, the D614G mutation, identified during the earlier stage of the pandemic, promotes spike binding to ACE2, leading to enhanced virus transmission (13, 14). Subsequently, the N501Y mutation found in the B.1.1.7, B.1.351, and B.1.1.28.1 spike proteins has increased the binding affinity between the receptor-binding domain (RBD) and ACE2, increasing viral fitness and infectivity (1, 15, 16). In addition, spike with the N501Y mutation has gained the ability to utilize mouse ACE2 as the receptor to infect the mouse, expanding its host range (12). In addition, K417N and E484K, found in the B.1.351 variant, contribute to evasion of neutralization by multiple monoclonal antibodies (17–19). Thus, as the COVID-19 pandemic continues, it is critical to closely monitor the emergence of new variants, as well as their impact on viral transmission, pathogenesis, and vaccine and therapeutic efficacies.

Recently, the numbers of COVID-19 cases and deaths in India have risen steeply, and the increased spread was associated with newly identified SARS-CoV-2 variants B.1.617 and B.1.618, which have mutated spike proteins (20, 21). B.1.617.1 (Kappa), which carries E154K in the N-terminal domain (NTD) of spike, L452R and E484Q mutations in the RBD of spike, and P681R in proximity to the furin cleavage site, has been designated a variant of interest (VOI) by the World Health Organization (WHO) (<https://www.who.int>). B.1.617.2 (Delta), which carries L452R and T478K mutations in the RBD of spike, as well as P681R, has been designated a VOC (<https://www.who.int>). B.1.618 harbors Δ 145–146 (deletion of the 145th and 146th residues) and an E484K mutation in the NTD and RBD, respectively. Indeed, some of the mutations in the Kappa, Delta, and B.1.618 have been found in other variants separately. For example, the L452R mutation has been spotted in the B.1.427 and B.1.429 variants, which have enhanced transmissibility and reduced sensitivity to vaccine-elicited antibodies (22, 23). T478K has been seen in Mexican variant B.1.1.519 (24). Also, the E484Q mutation is similar to the E484K mutation found in the B.1.351 variant, which exhibited reduced neutralization by convalescent-phase sera or monoclonal antibodies (17, 25–27). For the Kappa and Delta variants, this is the first time that L452R and E484Q (Kappa)/T478K (Delta) mutations have been found to coexist and the first time that P681R has been observed; for B.1.618, this is the first time the combination of Δ 145–146 in the NTD domain and E484K has been observed.

Here, we characterized the spike proteins of Kappa, Delta, and B.1.618 by their ability to utilize different ACE2 orthologs for cell entry and evaluated their sensitivity to convalescent-phase sera and soluble ACE2-Ig decoy receptor.

RESULTS

The spike proteins of Kappa, Delta, and B.1.618 gained increased binding affinity with human ACE2 and other orthologs. The rapid spread of the new emerging variants could be caused by the increased ability to enter the cell, since the variants harbor mutations in the spike proteins (Fig. 1A). To examine the biological impact of these

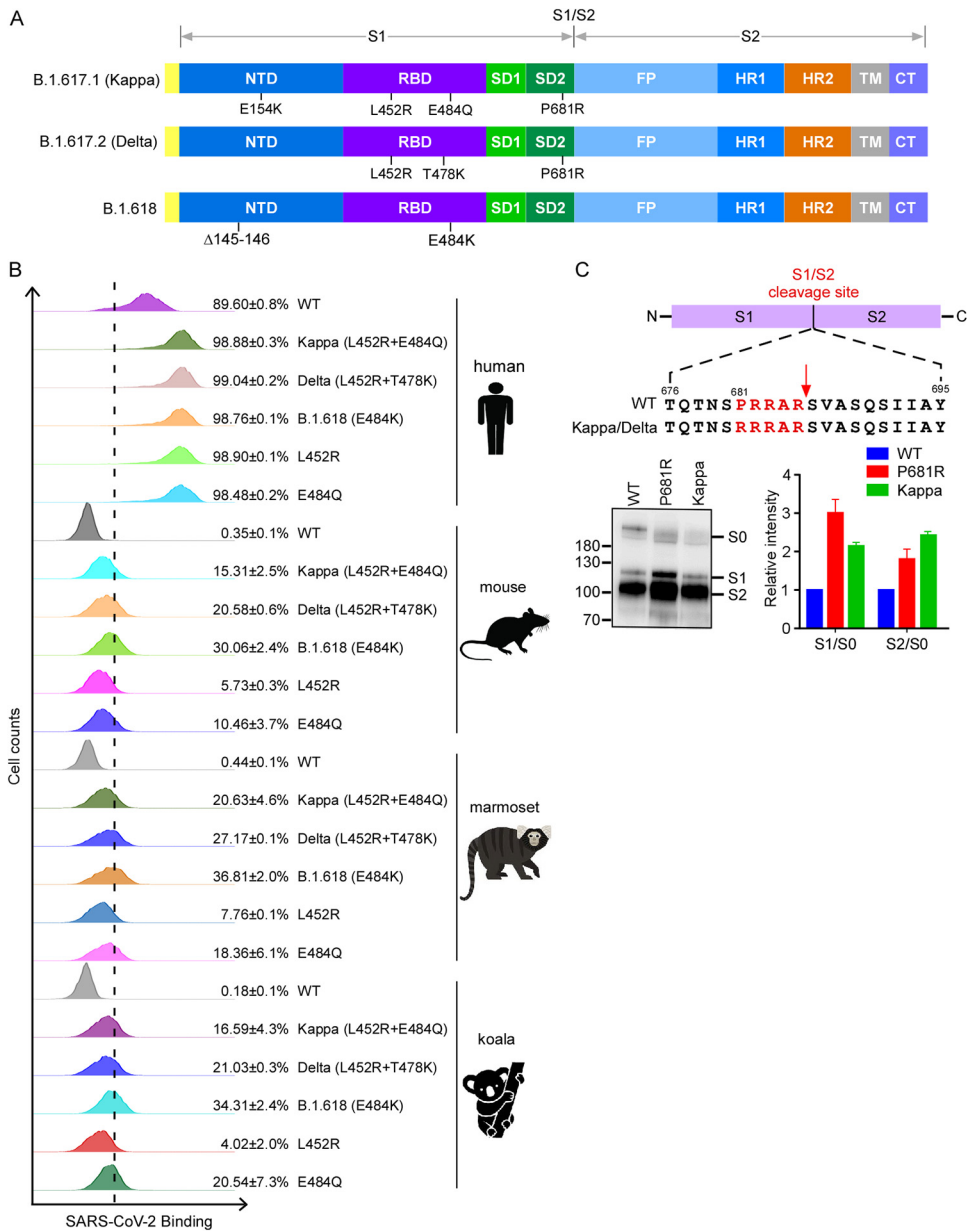


FIG 1 Binding of variants' spike proteins with ACE2 orthologs and spike protein processing. (A) Schematic overview of SARS-CoV-2 spike proteins of B.1.617.1 (Kappa), B.1.617.2 (Delta), and B.1.618, colored by domain. NTD, N-terminal domain; RBD, receptor binding domain; SD1, subdomain 1; SD2, subdomain 2; FP, fusion peptide; HR1, heptad repeat 1; HR2, heptad repeat 2; TM, transmembrane region; CT, cytoplasmic tail. (B) HeLa-ACE2 cells were incubated with recombinant RBD-His proteins bearing mutations of Kappa, Delta, and B.1.618 or an individual mutation. The binding of RBD-His with cells was analyzed by flow cytometry. Values are expressed as the percentage of cells positive for RBD-His among the ACE2-expressing cells (zsGreen1⁺ cells) and are shown as the means ± standard deviation (SD) from 3 biological replicates. This experiment was independently performed three times with similar results. (C) Immunoblot analysis of spike protein cleavage of pseudovirus of the Kappa and P681R variants using polyclonal antibodies against spike. Full-length spike (S0), S1, and S2 proteins are indicated. The ratio of S1 to S0 or S2 to S0 was quantitatively analyzed using ImageJ software. This experiment was repeated twice independently, and data were normalized to the WT (D614G) of the individual experiment.

mutations on binding with ACE2 cellular receptor, we employed a cell-based assay that uses flow cytometry to assess the binding of RBD of spike protein to human ACE2 (see Fig. S1A in the supplemental material). We cloned the cDNA of human ACE2 into a bicistronic lentiviral vector (pLVX-IRES-zsGreen1) that expresses the fluorescent protein zsGreen1 via an internal ribosome entry site (IRES) element and can be used to monitor

transduction efficiency. Next, wild-type (WT) or variant-derived RBD-His (a purified fusion protein consisting of the RBD and a polyhistidine tag at the C terminus) was incubated with HeLa cells transduced with the human ACE2. Binding of RBD-His to ACE2 was then quantified by flow cytometry (Fig. 1B; Fig. S1). As shown, the binding efficiencies of the RBDs of Kappa (L452R E484Q) (98.88%), Delta (L452R T478K) (99.04%), B.1.618 (E484K) (98.76%), L452R (98.90%), and E484Q (98.48%) were higher than that of the WT (89.6%), suggesting the RBDs of variants bind human ACE2 with a higher affinity (Fig. 1B).

To test whether the spike proteins of the variants are altered in binding with mouse, marmoset, and koala ACE2 orthologs, we incubated the recombinant RBD-His of the variants' spike proteins with HeLa cells expressing mouse, marmoset, or koala ACE2, and the binding of RBD-His to the ACE2 ortholog was quantified by flow cytometry (Fig. 1B; Fig. S1). WT RBD-His cannot bind with mouse, marmoset, or koala ACE2, as previously reported (7). In contrast, RBD-His of Kappa, Delta, and B.1.618 binds with mouse, marmoset, and koala ACE2 with various affinities, suggesting that these variants have evolved to gain the function for binding with nonhuman ACE2 orthologs.

Taken together, our results demonstrated that the spike proteins of Kappa, Delta, and B.1.618 have evolved to enhance their binding affinity with human ACE2. Remarkably, the spike proteins of these variants also gain the function to bind with mouse, marmoset, and koala ACE2.

P681R mutation in Kappa and Delta variants with enhanced spike protein cleavage and increased cell fusion activity. SARS-CoV-2 spike harbors a multibasic furin cleavage site (residues 681 to 686; PRRARS) at the S1/S2 junction, and the proteolytic processing of the spike by furin and TMPRSS2 proteases is important for SARS-CoV-2 infection (5, 28–31). Kappa and Delta variants contain a P681R substitution (Fig. 1A and C), potentially optimizing the furin cleavage site, which prompted us to examine the effect of the P681R substitution on furin cleavage. To do this, we produced murine leukemia virus (MLV) viral particles pseudotyped with WT, Kappa, or P681R spike. Viruses in the cell culture supernatants were harvested and concentrated for immunoblot analysis of spike protein cleavage by polyclonal antibody against spike protein (Fig. 1C). Interestingly, our data showed significantly increased cleavage of the full-length spike protein (S0) into the S1 and S2 fragments in Kappa spike and P681R spike pseudotyped viruses compared with WT spike. The cleaved S1/S0 ratio was 2.1-fold (Kappa) or 3.0-fold (P681R) higher than that of the WT, and the cleaved S2/S0 ratio was 2.4-fold (Kappa) or 1.8-fold (P681R) higher than that of the WT.

Interaction between spike protein and cellular receptor ACE2 mediated the fusion of virus with host cells, which was a prerequisite of virus entry into host cells (32). To better examine the cell fusion activities of the variants' spike proteins, we utilized a split green fluorescent protein (GFP) complementation-based cell fusion system to mimic the fusion of SARS-CoV-2-infected cells with ACE2-expressing cells (33, 34). We first derived the HEK293T cells transfected with cDNA expressing split GFP1 to -10 and spike (WT or variants) as the donor cells (HEK293T/GFP1-10/S), and cells transfected with cDNA expressing split GFP11 and human ACE2 as the acceptor cells (HEK293T/GFP11/ACE2). Then, the HEK293T/GFP1-10/S donor cells carrying various spike proteins were cocultured with HEK293T/GFP11/ACE2 acceptor cells at a 1:1 ratio. The donor cells and acceptor cells separately produce half of the reporter protein, generating a fluorescent signal only upon fusion of two cells (Fig. 2A). Microscopy showed that cell fusion occurred rapidly, as evidenced by the appearance of multinucleated GFP⁺ cells (syncytia) at 4 h after the coculture, and the syncytia grew in size as neighbor cells were incorporated in fused cells at 24 h (Fig. 2B). In addition, syncytium formation in the coculture system was dependent on the expression of spike and ACE2 (see Fig. S2 in the supplemental material). The extent of fusion was then quantified by measuring the GFP⁺ area: the spike proteins of the P681R, Kappa, and Delta variants were more active at cell fusion than the WT at both early and late time points (Fig. 2C).

Collectively, these results suggest that P681R substitution in the Kappa and Delta variants could enhance spike cleavage and promote cell fusion.

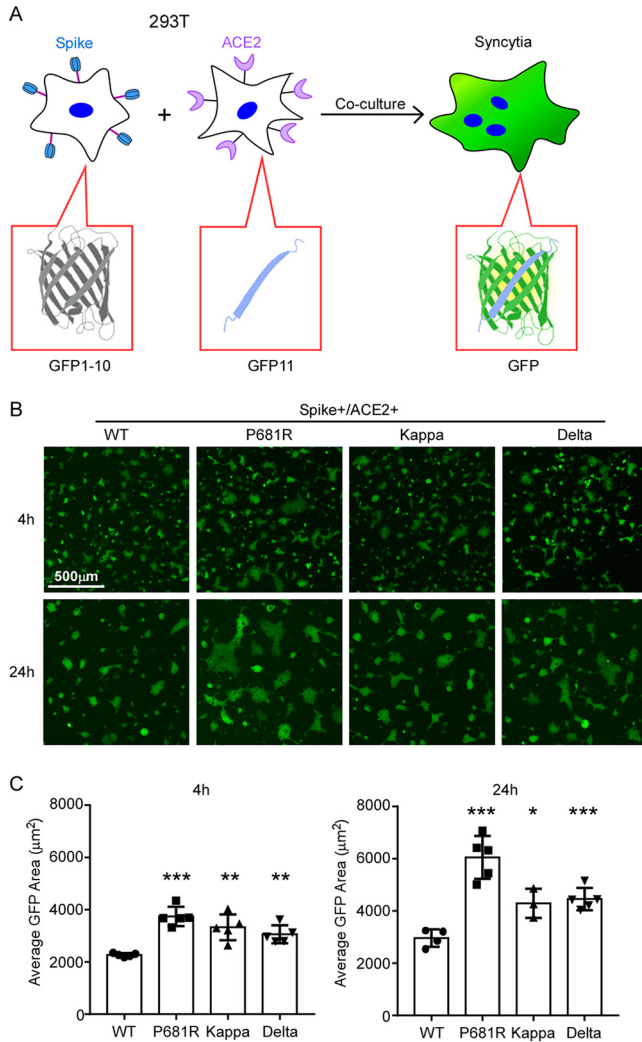


FIG 2 SARS-CoV-2 variant spike protein-mediated syncytium formation. (A) Schematic representation of syncytium formation between the donor cells expressing spike protein and split GFP and the acceptor cells expressing ACE2 receptor and split GFP. The images were taken at 4 h and 24 h by Nikon Ti2-U, with least three fields for each condition. The GFP-positive area and fused cell number were measured, and the average GFP areas of syncytia were measured by ImageJ. Results are means \pm SD from at least three fields per condition. Results are representative of at least three independent experiments. Scale bar, 500 μ m. Statistical analysis was performed by unpaired two-tail *t* test. *, *P* < 0.05; **, *P* < 0.01; ***, *P* < 0.001.

Characterization of cell entry driven by spike proteins of Kappa, Delta, and B.1.618. To further examine the biological impact of these mutations on cell entry, we produced pseudotyped virus particles containing a firefly luciferase reporter gene and expressing on their surface with the spike proteins of WT (D614G), Kappa, Delta, and B.1.618 variants. HeLa cells expressing human ACE2 (HeLa-human ACE2) were then inoculated with these pseudoparticles, and at 48 h postinoculation, the cells were lysed and the luciferase activity was monitored as a measure of virus entry (Fig. 3). Compared to WT spike, Delta and B.1.618 spike proteins gained an increased ability to mediate viral entry into HeLa-human ACE2 cells, which was contributed to by the T478K (Delta), P681R (Delta), Δ 145-146 (B.1.618), and E484K (B.1.618) variants. The spike protein of Kappa exhibited comparable ability to mediate viral entry: even an E484Q or P681R mutation in its spike could significantly promote viral entry individually.

SARS-CoV-2 has a broad host range, and its spike could utilize a diverse range of ACE2 orthologs for cell entry (7, 35). However, we and others previously found that SARS-CoV-2 spike has a limited binding affinity with mouse, New World monkey, or

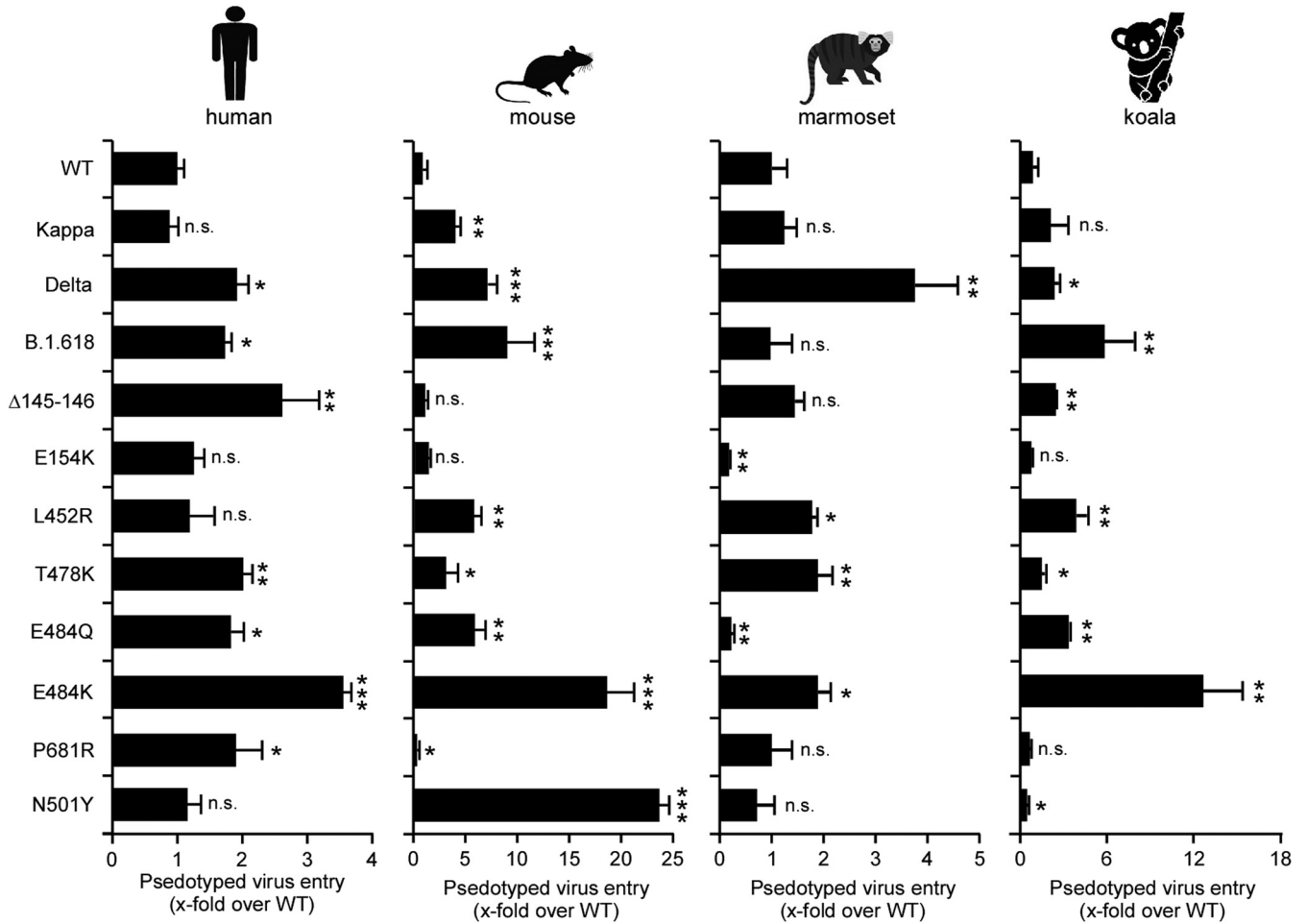


FIG 3 Spike proteins of variant-driven viral entry into HeLa cells expressing human, mouse, marmoset, or koala ACE2 orthologs. Cell entry of the virions pseudotyped with the WT, Kappa, Delta, or B.1.618 spike proteins or individual mutations of these variants' spike proteins was tested on HeLa cells expressing human, mouse, marmoset, or koala ACE2 orthologs. Luciferase activity was determined after 2 days of infection, and data were normalized to the WT (D614G) of the individual experiment. All infections were performed in triplicate, and the data are representative of three independent experiments (mean ± SD). n.s., no significance; *, $P < 0.05$; **, $P < 0.01$; ***, $P < 0.001$. Significance assessed by one-way ANOVA.

koala ACE2 and does not efficiently mediate virus entry into these species (3, 7, 36). We thus sought to evaluate the abilities of the variants' spike proteins to utilize these ACE2 proteins for cell entry. To this end, we produced virus pseudotyped with SARS-CoV-2 variant spike proteins with a single mutation or a combination of mutations. The HeLa cells expressing mouse, marmoset (New World monkey), or koala ACE2 orthologs were then inoculated with pseudoparticles, and luciferase activity was determined at 48 h postinoculation (Fig. 3). Our results showed that spike proteins from Kappa, Delta, and B.1.618 could significantly enhance cell entry into HeLa-mouse ACE2 cells, as a result of the T478K (Delta), E484Q (Kappa), and E484K (B.1.618) mutations. Besides HeLa-mouse ACE2, Delta also exhibited significantly enhanced cell entry into HeLa-marmoset and HeLa-koala cells, which are contributed to by L452R and T478K mutations. In contrast, Kappa did not increase cell entry into HeLa-marmoset or HeLa-koala cells, and B.1.618 only showed enhanced entry into HeLa-koala cells, which is attributable to E484K. In addition, the N501Y mutation in the spike has been demonstrated to have gained the ability to utilize mouse ACE2 for cell entry (12), and our data suggested that the N501Y mutant specifically gained the ability to utilize mouse ACE2 for cell entry, with an efficiency approximately 4-fold higher than that of Delta; however, the N501Y mutation has a negligible effect on utilization of marmoset or koala ACE2 for cell entry.

Taken together, our results demonstrated that the spike proteins of Kappa, Delta, or B.1.618 with distinct mutations have altered their ability to utilize ACE2 orthologs for

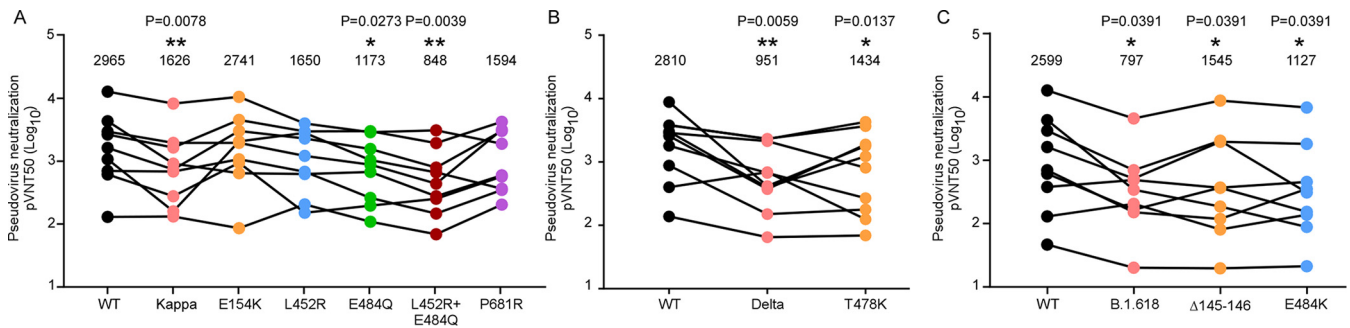


FIG 4 Reduced sensitivity of Kappa, Delta, and B.1.618 to neutralization of convalescent-phase sera. (A to C) MLV particles pseudotyped with the indicated spike proteins of Kappa, Delta, and B.1.618 or mutations as indicated were preincubated with serially diluted convalescent-phase sera, respectively. HeLa-ACE2 cells were incubated with these preincubated mixtures and analyzed 48 h later by measuring luciferase activity to calculate the plasma dilution factor leading to 50% reduction in spike protein-driven cell entry (50% neutralizing titer [NT₅₀]). The NT₅₀ of each serum against each pseudovirus (pVNT50) is presented, and identical serum samples are connected with lines. Statistical significance of differences between WT and variant spike proteins was analyzed by two-sided Friedman test with Dunn's multiple comparison. *, $P < 0.05$; **, $P < 0.01$. The pVNT50 of each sample was tested with two repeats.

cell entry. The Delta and B.1.618 variants gained an enhanced ability to use human ACE2 receptor for cell entry. Remarkably, the Delta variant gained the function to utilize mouse, New World monkey, or koala ACE2 orthologs, which cannot be engaged with WT virus, for cell entry.

Kappa, Delta, and B.1.618 variants exhibited resistance to neutralization by convalescent-phase serum, while remaining sensitive to an ACE2-based decoy receptor antiviral countermeasure. SARS-CoV-2 infection-elicited neutralizing antibodies target the spike protein, which is critical for protection from reinfection (37, 38). We hypothesized that mutations in the spike protein of the Kappa, Delta, and B.1.618 variants might contribute to the evasion of neutralizing antibodies. Therefore, we sought to determine the sensitivity of these variants to neutralization by convalescent-phase serum. We chose plasma from COVID-19 patients (see Tables S1, S2, and S3 in the supplemental material) and measured the neutralization activity of convalescent plasma against virions pseudotyped with single or combined mutations from the Kappa, Delta, and B.1.618 variants (Fig. 4A to C). To this end, we preincubated the serial-diluted convalescent-phase sera with virion pseudotyped with spike proteins as describe above, and subsequently tested on HeLa-human ACE2 cells. Cell entry of pseudotyped virion in the presence of convalescent plasma with various concentrations was assessed 48 h later by measurement of luciferase activities. The results showed that Kappa, Delta, and B.1.618 exhibited 1.8-, 3.0-, and 3.3-fold resistance to neutralization by convalescent-phase sera, respectively, which is conferred by E484Q, L452R E484Q, T478K, Δ145–146, and E484K (Fig. 4A, B, and C).

Previous studies have shown that ACE2-Ig (ACE2 fused with Fc recombinant protein) exhibited a potent antiviral effect against SARS-CoV-2 infection (35, 39). As the spike proteins of Kappa, Delta, and B.1.618 exhibited enhanced ACE2 binding affinity, it could be more sensitive to the inhibition by ACE2 decoy receptor. To this end, we used a SARS-CoV-2 transcription- and replication-competent virus-like particle (trVLP) cell culture system, which recapitulates the entire viral life cycle in Caco-2-N cells, to engineer the desired mutations in the spike proteins of Kappa, Delta, and B.1.618 variants into an SARS-CoV-2 isolate, Wuhan-Hu-1, with a D614G (WT) backbone, and examined the sensitivity of trVLP of Kappa, Delta, and B.1.618 to inhibition of ACE2-Ig. Specifically, we inoculated the Caco-2-N cells with WT, Kappa, Delta, or B.1.618 trVLP (multiplicity of infection [MOI] of 0.1) in the presence of ACE2-Ig at various concentrations. After 48 h, the cells were collected, and GFP expression was quantified as the proxy of virus infection by flow cytometry. ACE2-Ig could potentially inhibit WT, Kappa, Delta, and B.1.618 trVLP infection, with 50% inhibitory concentrations (IC₅₀s) of 21.05, 9.90, 15.81, and 15.77 ng/mL, indicating that the Kappa, Delta, and B.1.618 variants are still sensitive to inhibition by ACE2-Ig (Fig. 5A, B and C). In summary, the Kappa, Delta, and B.1.618 variants exhibited a reduced sensitivity to neutralization by convalescent-phase serum, while remaining sensitive to the ACE2 decoy receptor antiviral countermeasure.

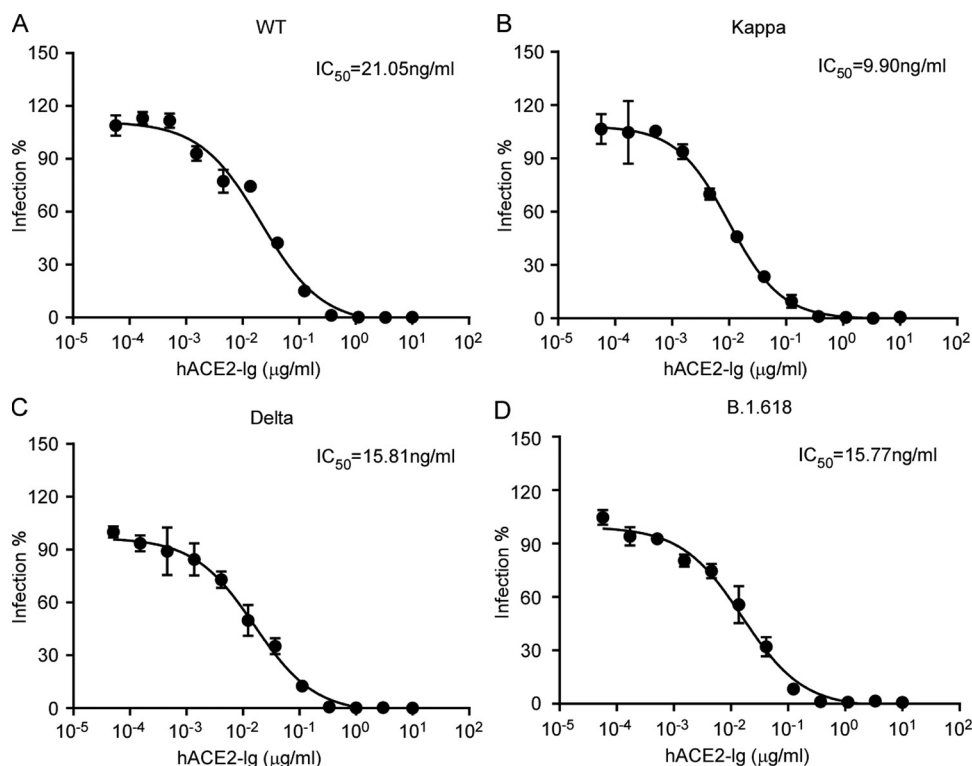


FIG 5 Inhibition of WT, Kappa, Delta, and B.1.618 by recombinant ACE2-Ig decoy receptor. Recombinant ACE2-Ig was diluted at the indicated concentrations. Viral entry was determined by assessing GFP expression 48 h postinfection of the WT (A) or Kappa (B), Delta (C) and B.1.618 (D) trVLP. The dilution factors leading to 50% reduction of trVLP entry were calculated as the IC₅₀ by using GraphPad Prism software. The data shown are representative of three independent experiments with similar results, and data points represent the mean ± SD in triplicate.

DISCUSSION

The emergence of SARS-CoV-2 variants imposes challenges on control of the COVID-19 pandemic (1, 40, 41). The recent surge in COVID-19 cases and mortalities in India is associated with new SARS-CoV-2 variants Kappa, Delta, and B.1.618 with mutated spike proteins (21). In this article, we characterized the biological properties of these new variants, including the efficiency of entry into cells, the binding affinities with human ACE2, as well as other orthologs, and the sensitivity to neutralization by convalescent plasma and recombinant ACE2-Ig decoy receptor.

We found that the Kappa variant did not show increased cell entry of HeLa-human ACE2 cells and had only slightly increased cell entry of HeLa-mouse ACE2 cells. The Delta variant had significantly increased cell entry of HeLa-human ACE2, HeLa-mouse ACE2, HeLa-marmoset ACE2, and HeLa-koala ACE2 cells; consistently, the Delta RBD bound human ACE2 with a higher affinity. Remarkably, Delta RBD gained the ability to bind with mouse, marmoset, and koala ACE2 orthologs, which exhibited limited binding affinity with WT RBD. The B.1.618 variant had dramatically increased cell entry of HeLa-human ACE2, HeLa-mouse ACE2, and HeLa-koala ACE2 cells, but not HeLa-marmoset ACE2 cells. Additionally, the P681R mutation in the spike proteins of Kappa and Delta variants enhanced the spike processing and cell fusion activities (Fig. 1C and Fig. 2A to C). Recent studies of infection with the Delta variant bearing P681R showed it could form large syncytia compared to other variants, further indicating that the P681R mutation in the furin cleavage site could enhance viral fusogenicity. As the furin cleavage site is critical for viral pathogenesis and transmission, the Kappa and Delta variants bearing the optimized furin cleavage site have potentially evolved increased pathogenicity and transmissibility, which urgently needs to be investigated. Remarkably, our results suggest that the Kappa, Delta, and B.1.618 variants have extended their usage of ACE2

orthologs into mice, koalas, and New World monkeys (Fig. 3), raising a potential risk of mice or other rodents becoming the reservoirs for SARS-CoV-2, and the virus could potentially spill back to humans as the mice live close to humans.

SARS-CoV-2 variants Kappa, Delta, and B.1.618 exhibited reduced sensitivity to neutralization by polyclonal antibodies in the serum from individuals previously infected with SARS-CoV-2 (Fig. 4A to C). Our analysis suggests that the immune escape is mainly conferred by the E484Q, T484K, Δ 145–146, and E484K mutations: these new variants must be further surveyed to avoid fast spread, and their presence might raise alerts if they might be considered likely to soon contribute to accelerating the spread of the virus in human populations. Thus, our findings highlight the critical need for broad-spectrum neutralizing antibodies insensitive to substitutions arising in VOC or VOI. In addition, we further demonstrated that the ACE2 decoy receptor-based antiviral strategy is an alternative countermeasure against the VOC, as the VOC Kappa and B.1.618 exhibited increased binding with human ACE2 (1, 41). Our results show that recombinant ACE2-Ig protein could inhibit Kappa, Delta, and B.1.618 infection with efficacy comparable to or better than that of the WT (Fig. 5A to D), which is consistent with the results that Kappa, Delta, and B.1.618 spike proteins exhibited increased binding affinity with human ACE2 (Fig. 1B). In addition, it has been demonstrated that human ACE2 peptidase activity and viral receptor activity could be uncoupled; thus, it is possible that enzymatically inactivated ACE2 could be developed as an antiviral in clinics to avoid the potential ACE2 side effects mediated by its enzymatic activity.

New variants of concern will continue to emerge as the COVID-19 pandemic persists, which highlights the importance of genomic surveillance for the early identification of future variants. The potential of variants to escape naturally induced and vaccine-elicited immunity makes the development of next-generation vaccines that elicit broadly neutralizing activity against current and future variants a priority (22, 25, 42). In addition, the suppression of viral replication through both public health measures and the equitable distribution of vaccines, increasing the proportion of the population immunized with the current safe and effective authorized vaccines, is critical to minimize the risk of emergence of new variants. Also, the development of broad-spectrum antivirals, especially against diverse SARS-CoV-2 variants, is therefore of continued significance.

MATERIALS AND METHODS

Cell culture. HEK293T (American Tissue Culture Collection, ATCC, Manassas, VA, CRL-3216), Vero E6 (Cell Bank of the Chinese Academy of Sciences, Shanghai, China), and A549 (ATCC) cells were maintained in Dulbecco's modified Eagle's medium (DMEM) (Gibco, NY, USA) supplemented with 10% (vol/vol) fetal bovine serum (FBS), 10 mM HEPES, 1 mM sodium pyruvate, 1 \times nonessential amino acids, and 50 IU/mL penicillin-streptomycin in a humidified 5% (vol/vol) CO₂ incubator at 37°C. Cells were tested routinely and found to be free of mycoplasma contamination.

Plasmids. The cDNAs encoding the ACE2 orthologs were synthesized by GenScript and cloned into the pLVX-IRES-zsGreen1 vector (catalog no. 632187; Clontech Laboratories, Inc.) with a C-terminal FLAG tag. Spike mutants were generated by Quikchange (Stratagene) site-directed mutagenesis. All constructs were verified by Sanger sequencing.

Lentivirus production. Vesicular stomatitis virus G protein (VSV-G) pseudotyped lentiviruses expressing ACE2 orthologs tagged with FLAG at the C terminus were produced by transient cotransfection of the third-generation packaging plasmids pMD2G (Addgene catalog no. 12259) and psPAX2 (Addgene catalog no. 12260) and the transfer vector with VigoFect DNA transfection reagent (Vigorous) into HEK293T cells. The medium was changed 12 h posttransfection. Supernatants were collected at 24 and 48 h after transfection, pooled, passed through a 0.45- μ m-pore filter, and frozen at -80°C .

Surface ACE2 binding with RBD-His assay. HeLa cells were transduced with lentiviruses expressing the ACE2 variants for 48 h. The cells were collected with TrypLE (Thermo catalog no. 12605010) and washed twice with cold phosphate-buffered saline (PBS). Live cells were incubated with the recombinant proteins' RBD-His with mutations (Sino Biological catalog no. 40592-V08B, 40592-V08H88, 40592-V08H90, 40592-V08H84, 40592-V08H28, and 40592-V08H81) at 1 $\mu\text{g}/\text{mL}$ at 4°C for 30 min. After washing, cells were stained with Anti-His-phycoerythrin (PE) (clone GG11-8F3.5.1; Miltenyi Biotec catalog no. 130-120-787) for 30 min at 4°C. Cells were then washed twice and subjected to flow cytometry analysis (Attune NxT; Thermo). Binding efficiencies are expressed as the percentage of cells positive for RBD-His among the zsGreen-positive cells (ACE2-expressing cells).

Cell-cell fusion assay. For HEK293T donor cells (HEK293T/GFP1–10/S), the HEK293T cells were grown to 50% confluence in a 24-well plate and transfected with 0.5 μg pcDNA3.1-GFP1–10 and 0.5 μg pcDNA-SARS-CoV-2 spike (WT or variant). For HEK293T acceptor cells (HEK293T/GFP11/ACE2), the HEK293T cells in

a 24-well plate were transfected with 0.5 μ g pcDNA3.1-GFP11 and 0.5 μ g pLVX-human ACE2-IRES-Puro. After 12 h, the donor cell and acceptor cell populations were trypsinized and seeded together into 24-well plates at a 1:1 ratio. The cells were then left to fuse, and fluorescence images were taken at the indicated time point using a Nikon Ti2-U with at least three fields for each condition.

Production of SARS-CoV-2 pseudotyped virus, determination of viral entry efficiency, and analysis of spike protein cleavage. Pseudoviruses were produced in HEK293T cells by cotransfecting the retroviral vectors pTG-MLV-Fluc, pTG-MLV-Gag-pol, and pcDNA3.1 expressing SARS-CoV-2 spike gene or VSV-G (pMD2.G; Addgene catalog no. 12259) by using VigoFect (Vigorous Biotechnology). At 48 h posttransfection, the cell culture medium was collected for centrifugation at 3,500 rpm for 10 min, and then the supernatant was subsequently aliquoted and stored at -80°C for further use. Virus entry was assessed by transduction of pseudoviruses in cells expressing an ACE2 ortholog in 48-well plates. After 48 h, intracellular luciferase activity was determined using the Promega luciferase assay system (Promega catalog no. E1500) according to the manufacturer's instructions. Luminescence was recorded on a GloMax Discover system (Promega). To analyze the spike protein cleavage, the concentrated pseudoviruses were produced by ultracentrifugation at $100,000 \times g$ for 2 h over a 20% sucrose cushion. Western blot detection of SARS-CoV-2 spike protein was performed using a polyclonal spike antibody (Sino Biological catalog no. 40589-T62).

Human convalescent-phase serum and neutralization of pseudotyped virion particles. We obtained convalescent-phase serum from COVID-19 patients (Tables S1, S2, and S3) more than 1 month after documented SARS-CoV-2 infection in the spring of 2020. Each plasma sample was heat inactivated (56°C , 30 min) and then assayed for neutralization against WT or Kappa, Delta, and B.1.618 variant pseudoviruses. For neutralization experiments, 5 protein-bearing pseudotyped virion particles were preincubated for 1 h at 37°C with diluted plasma samples obtained from convalescent COVID-19 patients, before the mixtures were inoculated onto HeLa-ACE2 cells. Transduction efficiency was determined at 48 h post-inoculation. This study was approved by the Institution Review Board of Tsinghua University (20210040).

Recombinant ACE2-Ig protein expression and purification. ACE2-Ig, a recombinant Fc fusion protein of soluble human ACE2 (residues Gln18 to Ser740) was expressed in 293F cells and purified using protein A affinity chromatography as described in our previous study (35).

Production of SARS-CoV-2 trVLP. The desired mutations in the spike proteins of Kappa, Delta, and B.1.618 variants in an SARS-CoV-2 isolate, Wuhan-Hu-1, with a D614G (WT) backbone and the trVLP, were generated as previously described (43).

Statistical analysis. One-way analysis of variance (ANOVA) with Tukey's honestly significant difference (HSD) test was used to test for statistical significance of differences between the different group parameters. *P* values of <0.05 were considered statistically significant.

SUPPLEMENTAL MATERIAL

Supplemental material is available online only.

FIG S1, PDF file, 2.4 MB.

FIG S2, PDF file, 0.1 MB.

TABLE S1, XLSX file, 0.01 MB.

TABLE S2, XLSX file, 0.01 MB.

TABLE S3, XLSX file, 0.01 MB.

ACKNOWLEDGMENTS

We thank Jenna M. Gaska for suggestions and revision of the manuscript. We are grateful to other members of the Ding lab for critical discussions and comments on the manuscript.

This work was supported by the National Natural Science Foundation of China (32070153), Tsinghua University Spring Breeze Fund (2021Z99CFY030), Beijing Municipal Natural Science Foundation (M21001), Advanced Customer Cultivation Project of Wuhan National Biosafety Laboratory, Chinese Academy of Sciences (2021ACCP-MS03), and the Start-up Foundation of Tsinghua University (53332101319).

REFERENCES

1. Wu A, Wang L, Zhou H-Y, Ji C-Y, Xia SZ, Cao Y, Meng J, Ding X, Gold S, Jiang T, Cheng G. 2021. One year of SARS-CoV-2 evolution. *Cell Host Microbe* 29: 503–507. <https://doi.org/10.1016/j.chom.2021.02.017>.
2. Zhou P, Yang X-L, Wang X-G, Hu B, Zhang L, Zhang W, Si H-R, Zhu Y, Li B, Huang C-L, Chen H-D, Chen J, Luo Y, Guo H, Jiang R-D, Liu M-Q, Chen Y, Shen X-R, Wang X, Zheng X-S, Zhao K, Chen Q-J, Deng F, Liu L-L, Yan B, Zhan F-X, Wang Y-Y, Xiao G-F, Shi Z-L. 2020. A pneumonia outbreak associated with a new coronavirus of probable bat origin. *Nature* 579: 270–273. <https://doi.org/10.1038/s41586-020-2012-7>.
3. Wu F, Zhao S, Yu B, Chen Y-M, Wang W, Song Z-G, Hu Y, Tao Z-W, Tian J-H, Pei Y-Y, Yuan M-L, Zhang Y-L, Dai F-H, Liu Y, Wang Q-M, Zheng J-J, Xu L, Holmes EC, Zhang Y-Z. 2020. A new coronavirus associated with human respiratory disease in China. *Nature* 579:265–269. <https://doi.org/10.1038/s41586-020-2008-3>.
4. Wang C, Horby PW, Hayden FG, Gao GF. 2020. A novel coronavirus outbreak of global health concern. *Lancet* 395:470–473. [https://doi.org/10.1016/S0140-6736\(20\)30185-9](https://doi.org/10.1016/S0140-6736(20)30185-9).
5. Hoffmann M, Kleine-Weber H, Schroeder S, Krüger N, Herrler T, Erichsen S, Schiergens TS, Herrler G, Wu N-H, Nitsche A, Müller MA, Drosten C, Pöhlmann S. 2020. SARS-CoV-2 cell entry depends on ACE2 and TMPRSS2 and is blocked by a clinically proven protease inhibitor. *Cell* 181:271–280.e278. <https://doi.org/10.1016/j.cell.2020.02.052>.

6. Lu G, Wang Q, Gao GF. 2015. Bat-to-human: spike features determining 'host jump' of coronaviruses SARS-CoV, MERS-CoV, and beyond. *Trends Microbiol* 23:468–478. <https://doi.org/10.1016/j.tim.2015.06.003>.
7. Liu Y, Hu G, Wang Y, Ren W, Zhao X, Ji F, Zhu Y, Feng F, Gong M, Ju X, Zhu Y, Cai X, Lan J, Guo J, Xie M, Dong L, Zhu Z, Na J, Wu J, Lan X, Xie Y, Wang X, Yuan Z, Zhang R, Ding Q. 2021. Functional and genetic analysis of viral receptor ACE2 orthologs reveals a broad potential host range of SARS-CoV-2. *Proc Natl Acad Sci U S A* 118:e2025373118. <https://doi.org/10.1073/pnas.2025373118>.
8. Ju B, Zhang Q, Ge J, Wang R, Sun J, Ge X, Yu J, Shan S, Zhou B, Song S, Tang X, Yu J, Lan J, Yuan J, Wang H, Zhao J, Zhang S, Wang Y, Shi X, Liu L, Zhao J, Wang X, Zhang Z, Zhang L. 2020. Human neutralizing antibodies elicited by SARS-CoV-2 infection. *Nature* 584:115–119. <https://doi.org/10.1038/s41586-020-2380-z>.
9. Krammer F. 2020. SARS-CoV-2 vaccines in development. *Nature* 586:516–527. <https://doi.org/10.1038/s41586-020-2798-3>.
10. Jiang R-D, Liu M-Q, Chen Y, Shan C, Zhou Y-W, Shen X-R, Li Q, Zhang L, Zhu Y, Si H-R, Wang Q, Min J, Wang X, Zhang W, Li B, Zhang H-J, Baric RS, Zhou P, Yang X-L, Shi Z-L. 2020. Pathogenesis of SARS-CoV-2 in transgenic mice expressing human angiotensin-converting enzyme 2. *Cell* 182:50–58.e58. <https://doi.org/10.1016/j.cell.2020.05.027>.
11. Leist SR, Dinnon KH, Schäfer A, Tse LV, Okuda K, Hou YJ, West A, Edwards CE, Sanders W, Fritch EJ, Gully KL, Scobey T, Brown AJ, Sheahan TP, Moorman NJ, Boucher RC, Gralinski LE, Montgomery SA, Baric RS. 2020. A mouse-adapted SARS-CoV-2 induces acute lung injury (ALI) and mortality in standard laboratory mice. *Cell* 183:1070–1085.e12. <https://doi.org/10.1016/j.cell.2020.09.050>.
12. Gu H, Chen Q, Yang G, He L, Fan H, Deng Y-Q, Wang Y, Teng Y, Zhao Z, Cui Y, Li Y, Li X-F, Li J, Zhang N-N, Yang X, Chen S, Guo Y, Zhao G, Wang X, Luo D-Y, Wang H, Yang X, Li Y, Han G, He Y, Zhou X, Geng S, Sheng X, Jiang S, Sun S, Qin C-F, Zhou Y. 2020. Adaptation of SARS-CoV-2 in BALB/c mice for testing vaccine efficacy. *Science* 369:1603–1607. <https://doi.org/10.1126/science.abc4730>.
13. Korber B, Fischer WM, Gnanakaran S, Yoon H, Theiler J, Abfalterer W, Hengartner N, Giorgi EE, Bhattacharya T, Foley B, Hastie KM, Parker MD, Partridge DG, Evans CM, Freeman TM, de Silva TI, McDanel C, Perez LG, Tang H, Moon-Walker A, Whelan SP, LaBranche CC, Saphire EO, Montefiori DC, Sheffield COVID-19 Genomics Group. 2020. Tracking changes in SARS-CoV-2 spike: evidence that D614G increases infectivity of the COVID-19 virus. *Cell* 182:812–827.e819. <https://doi.org/10.1016/j.cell.2020.06.043>.
14. Plante JA, Liu Y, Liu J, Xia H, Johnson BA, Lokugamage KG, Zhang X, Muruato AE, Zou J, Fontes-Garfias CR, Mirchandani D, Scharton D, Billelo JP, Ku Z, An Z, Kalveram B, Freiberg AN, Menachery VD, Xie X, Plante KS, Weaver SC, Shi P-Y. 2021. Spike mutation D614G alters SARS-CoV-2 fitness. *Nature* 592:116–121. <https://doi.org/10.1038/s41586-020-2895-3>.
15. Peacock TP, Penrice-Randal R, Hiscox JA, Barclay WS. 2021. SARS-CoV-2 one year on: evidence for ongoing viral adaptation. *J Gen Virol* 102:001584. <https://doi.org/10.1099/jgv.0.001584>.
16. Starr TN, Greaney AJ, Hilton SK, Ellis D, Crawford KHD, Dingens AS, Navarro MJ, Bowen JE, Tortorici MA, Walls AC, King NP, Veesler D, Bloom JD. 2020. Deep mutational scanning of SARS-CoV-2 receptor binding domain reveals constraints on folding and ACE2 binding. *Cell* 182:1295–1310.e1220. <https://doi.org/10.1016/j.cell.2020.08.012>.
17. Zhou D, Dejnirattisai W, Supasa P, Liu C, Mentzer AJ, Ginn HM, Zhao Y, Duyvesteyn HME, Tuekprakhon A, Nutalai R, Wang B, Paesen GC, Lopez-Camacho C, Slon-Campos J, Hallis B, Coombes N, Bewley K, Charlton S, Walter TS, Skelly D, Lumley SF, Dold C, Levin R, Dong T, Pollard AJ, Knight JC, Crook D, Lambe T, Clutterbuck E, Bibi S, Flaxman A, Bittaye M, Belij-Rammerstorfer S, Gilbert S, James W, Carroll MW, Klenerman P, Barnes E, Dunachie SJ, Fry EE, Mongkolsapaya J, Ren J, Stuart DI, Screaton GR. 2021. Evidence of escape of SARS-CoV-2 variant B.1.351 from natural and vaccine-induced sera. *Cell* 184:2348–2361.e2346. <https://doi.org/10.1016/j.cell.2021.02.037>.
18. Garcia-Beltran WF, Lam EC, St Denis K, Nitido AD, Garcia ZH, Hauser BM, Feldman J, Pavlovic MN, Gregory DJ, Poznansky MC, Sigal A, Schmidt AG, lafrate AJ, Naranbhai V, Balazs AB. 2021. Multiple SARS-CoV-2 variants escape neutralization by vaccine-induced humoral immunity. *Cell* 184:2372–2383.e9. <https://doi.org/10.1016/j.cell.2021.03.013>.
19. Harvey WT, Carabelli MN, Jackson B, Gupta RK, Thomson EC, Harrison EM, Ludden C, Reeve R, Rambaut A, Peacock SJ, Robertson DL, COVID-19 Genomics UK (COG-UK) Consortium. 2021. SARS-CoV-2 variants, spike mutations and immune escape. *Nat Rev Microbiol* 19:409–424. <https://doi.org/10.1038/s41579-021-00573-0>.
20. Cherian S, Potdar V, Jadhav S, Yadav P, Gupta N, Das M, Das S, Agarwal A, Singh S, Abraham P, Panda S, Mande S, Swarup R, Bhargava B, Bhushan R, NIC Team, INSACOG Consortium. 2021. Convergent evolution of SARS-CoV-2 spike mutations, L452R, E484Q and P681R, in the second wave of COVID-19 in Maharashtra, India. *bioRxiv* <https://www.biorxiv.org/content/10.1101/2021.04.22.440932v1>.
21. Tada T, Zhou H, Dcosta BM, Samanovic MI, Mulligan MJ, Landau NR. 2021. The spike proteins of SARS-CoV-2 B.1.617 and B.1.618 variants identified in India provide partial resistance to vaccine-elicited and therapeutic monoclonal antibodies. *bioRxiv* <https://www.biorxiv.org/content/10.1101/2021.05.14.444076v1>.
22. McCallum M, Bassi J, De Marco A, Chen A, Walls AC, Di Iulio J, Tortorici MA, Navarro M-J, Silacci-Fregni C, Saliba C, Agostini M, Pinto D, Culap K, Bianchi S, Jaconi S, Camerini E, Bowen JE, Tilles SW, Pizzuto MS, Bernasconi Guastalla S, Bona G, Franzetti Pellanda A, Garzoni C, Van Voorhis WE, Rosen LE, Snell G, Telenti A, Virgin HW, Piccoli L, Corti D, Veesler D. 2021. SARS-CoV-2 immune evasion by variant B.1.427/B.1.429. *bioRxiv* <https://www.biorxiv.org/content/10.1101/2021.03.31.437925v1>.
23. Motozono C, Toyoda M, Zahradnik J, Saito A, Nasser H, Tan TS, Ngare I, Kimura I, Uriu K, Kosugi Y, Yue Y, Shimizu R, Ito J, Torii S, Yonekawa A, Shimono N, Nagasaki Y, Minami R, Taya T, Sekiya N, Fukuhara T, Matsuurra Y, Schreiber G, Ikeda T, Nakagawa S, Ueno T, Sato K, Genotype to Phenotype Japan (G2P-Japan) Consortium. 2021. SARS-CoV-2 spike L452R variant evades cellular immunity and increases infectivity. *Cell Host Microbe* 29:1124–1136.e1111. <https://doi.org/10.1016/j.chom.2021.06.006>.
24. Di Giacomo S, Mercatelli D, Rakhimov A, Giorgi FM. 2021. Preliminary report on severe acute respiratory syndrome coronavirus 2 (SARS-CoV-2) spike mutation T478K. *J Med Virol* 93:5638–5643. <https://doi.org/10.1002/jmv.27062>.
25. Planas D, Bruel T, Grzelak L, Guivel-Benhassine F, Staropoli I, Porrot F, Planchais C, Buchrieser J, Rajah MM, Bishop E, Albert M, Donati F, Prot M, Behillil S, Enouf V, Maquart M, Smati-Lafarge M, Varon E, Schortgen F, Yahyaoui L, Gonzalez M, De Sèze J, Péré H, Veyer D, Sève A, Simon-Lorière E, Fafi-Kremer S, Stefic K, Mouquet H, Hocqueloux L, van der Werf S, Prazuck T, Schwartz O. 2021. Sensitivity of infectious SARS-CoV-2 B.1.1.7 and B.1.351 variants to neutralizing antibodies. *Nat Med* 27:917–924. <https://doi.org/10.1038/s41591-021-01318-5>.
26. Cele S, Gazy I, Jackson L, Hwa S-H, Tegally H, Lustig G, Giandhari J, Pillay S, Wilkinson E, Naidoo Y, Karim F, Ganga Y, Khan K, Bernstein M, Balazs AB, Gosnell BI, Hanekom W, Moosa M-YS, Lessells RJ, de Oliveira T, Sigal A, Network for Genomic Surveillance in South Africa. 2021. Escape of SARS-CoV-2 501Y.V2 from neutralization by convalescent plasma. *Nature* 593:142–146. <https://doi.org/10.1038/s41586-021-03471-w>.
27. Edara VV, Norwood C, Floyd K, Lai L, Davis-Gardner ME, Hudson WH, Mantus G, Nyhoff LE, Adelman MW, Fineman R, Patel S, Byram R, Gomes DN, Michael G, Abdullahi H, Beydoun N, Panganiban B, McNair N, Hellmeister K, Pitts J, Winters J, Kleinhenz J, Usher J, O'Keefe JB, Piantadosi A, Waggoner JJ, Babiker A, Stephens DS, Anderson EJ, Edupuganti S, Roupael N, Ahmed R, Wrammert J, Suthar MS. 2021. Infectious and vaccine-induced antibody binding and neutralization of the B.1.351 SARS-CoV-2 variant. *Cell Host Microbe* 29:516–521.e513. <https://doi.org/10.1016/j.chom.2021.03.009>.
28. Papa G, Mallery DL, Albecka A, Welch LG, Cattin-Ortolá J, Luptak J, Paul D, McMahon HT, Goodfellow IG, Carter A, Munro S, James LC. 2021. Furin cleavage of SARS-CoV-2 spike promotes but is not essential for infection and cell-cell fusion. *PLoS Pathog* 17:e1009246. <https://doi.org/10.1371/journal.ppat.1009246>.
29. Walls AC, Park Y-J, Tortorici MA, Wall A, McGuire AT, Veesler D. 2020. Structure, function, and antigenicity of the SARS-CoV-2 spike glycoprotein. *Cell* 181:281–292.e286. <https://doi.org/10.1016/j.cell.2020.02.058>.
30. Zhu Y, Feng F, Hu G, Wang Y, Yu Y, Zhu Y, Xu W, Cai X, Sun Z, Han W, Ye R, Qu D, Ding Q, Huang X, Chen H, Xu W, Xie Y, Cai Q, Yuan Z, Zhang R. 2021. A genome-wide CRISPR screen identifies host factors that regulate SARS-CoV-2 entry. *Nat Commun* 12:961. <https://doi.org/10.1038/s41467-021-21213-4>.
31. Matsuyama S, Nao N, Shirato K, Kawase M, Saito S, Takayama I, Nagata N, Sekizuka T, Katoh H, Kato F, Sakata M, Tahara M, Kutsuna S, Ohmagari N, Kuroda M, Suzuki T, Kageyama T, Takeda M. 2020. Enhanced isolation of SARS-CoV-2 by TMPRSS2-expressing cells. *Proc Natl Acad Sci U S A* 117:7001–7003. <https://doi.org/10.1073/pnas.2002589117>.
32. Baggen J, Vanstreels E, Jansen S, Daelemans D. 2021. Cellular host factors for SARS-CoV-2 infection. *Nat Microbiol* 6:1219–1232. <https://doi.org/10.1038/s41564-021-00958-0>.

33. Kamiyama D, Sekine S, Barsi-Rhyné B, Hu J, Chen B, Gilbert LA, Ishikawa H, Leonetti MD, Marshall WF, Weissman JS, Huang B. 2016. Versatile protein tagging in cells with split fluorescent protein. *Nat Commun* 7:11046. <https://doi.org/10.1038/ncomms11046>.
34. Buchrieser J, Dufloo J, Hubert M, Monel B, Planas D, Rajah MM, Planchais C, Porrot F, Guivel-Benhassine F, Van der Werf S, Casartelli N, Mouquet H, Bruel T, Schwartz O. 2020. Syncytia formation by SARS-CoV-2-infected cells. *EMBO J* 39:e106267. <https://doi.org/10.15252/emboj.2020106267>.
35. Li Y, Wang H, Tang X, Fang S, Ma D, Du C, Wang Y, Pan H, Yao W, Zhang R, Zou X, Zheng J, Xu L, Farzan M, Zhong G. 2020. SARS-CoV-2 and three related coronaviruses utilize multiple ACE2 orthologs and are potentially blocked by an improved ACE2-Ig. *J Virol* 94:e01283-20. <https://doi.org/10.1128/JVI.01283-20>.
36. Ren W, Zhu Y, Wang Y, Shi H, Yu Y, Hu G, Feng F, Zhao X, Lan J, Wu J, Kenney DJ, Douam F, Tong Y, Zhong J, Xie Y, Wang X, Yuan Z, Zhou D, Zhang R, Ding Q. 2021. Comparative analysis reveals the species-specific genetic determinants of ACE2 required for SARS-CoV-2 entry. *PLoS Pathog* 17:e1009392. <https://doi.org/10.1371/journal.ppat.1009392>.
37. Cao Y, Su B, Guo X, Sun W, Deng Y, Bao L, Zhu Q, Zhang X, Zheng Y, Geng C, Chai X, He R, Li X, Lv Q, Zhu H, Deng W, Xu Y, Wang Y, Qiao L, Tan Y, Song L, Wang G, Du X, Gao N, Liu J, Xiao J, Su X-D, Du Z, Feng Y, Qin C, Qin C, Jin R, Xie XS. 2020. Potent neutralizing antibodies against SARS-CoV-2 identified by high-throughput single-cell sequencing of convalescent patients' B cells. *Cell* 182:73–84.e16. <https://doi.org/10.1016/j.cell.2020.05.025>.
38. Hassan AO, Case JB, Winkler ES, Thackray LB, Kafai NM, Bailey AL, McCune BT, Fox JM, Chen RE, Alsoussi WB, Turner JS, Schmitz AJ, Lei T, Shrihari S, Keeler SP, Fremont DH, Greco S, McCray PB, Perlman S, Holtzman MJ, Ellebedy AH, Diamond MS. 2020. A SARS-CoV-2 infection model in mice demonstrates protection by neutralizing antibodies. *Cell* 182:744–753.e744. <https://doi.org/10.1016/j.cell.2020.06.011>.
39. Monteil V, Kwon H, Prado P, Hagelkrüys A, Wimmer RA, Stahl M, Leopoldi A, Garreta E, Hurtado Del Pozo C, Prosper F, Romero JP, Wirnsberger G, Zhang H, Slutsky AS, Conder R, Montserrat N, Mirazimi A, Penninger JM. 2020. Inhibition of SARS-CoV-2 infections in engineered human tissues using clinical-grade soluble human ACE2. *Cell* 181:905–913.e907. <https://doi.org/10.1016/j.cell.2020.04.004>.
40. Rochman ND, Wolf YI, Faure G, Mutz P, Zhang F, Koonin EV. 2021. Ongoing global and regional adaptive evolution of SARS-CoV-2. *Proc Natl Acad Sci U S A* 118:e2104241118. <https://doi.org/10.1073/pnas.2104241118>.
41. Zhou H-Y, Ji C-Y, Fan H, Han N, Li X-F, Wu A, Qin C-F. 2021. Convergent evolution of SARS-CoV-2 in human and animals. *Protein Cell* 12:832–835. <https://doi.org/10.1007/s13238-021-00847-6>.
42. Planas D, Veyer D, Baidaliuk A, Staropoli I, Guivel-Benhassine F, Rajah MM, Planchais C, Porrot F, Robillard N, Puech J, Prot M, Gallais F, Gantner P, Velay A, Le Guen J, Kassis-Chikhani N, Edriss D, Belec L, Seve A, Courtellemont L, Péré H, Hocqueloux L, Fafi-Kremer S, Prazuck T, Mouquet H, Bruel T, Simon-Lorière E, Rey FA, Schwartz O. 2021. Reduced sensitivity of SARS-CoV-2 variant Delta to antibody neutralization. *Nature* 596:276–280. <https://doi.org/10.1038/s41586-021-03777-9>.
43. Ju X, Zhu Y, Wang Y, Li J, Zhang J, Gong M, Ren W, Li S, Zhong J, Zhang L, Zhang QC, Zhang R, Ding Q. 2021. A novel cell culture system modeling the SARS-CoV-2 life cycle. *PLoS Pathog* 17:e1009439. <https://doi.org/10.1371/journal.ppat.1009439>.